

Character of magnetic instabilities in CaFe_2As_2

G. D. Samolyuk* and V. P. Antropov

Condensed Matter Physics, Ames Laboratory, Ames, Iowa 50011, USA

(Received 7 October 2008; published 19 February 2009)

The density-functional spin susceptibility has been analyzed in different phases of CaFe_2As_2 and compared with similar data for pure d metals. The conditions for the “no local-moment” itinerant state with large frustrations are found for the “collapsed” phase. This itineracy determines the instability versus the incommensurate magnetic order for the narrow region of wave vectors. For the ambient pressure phase, the local moments on Fe atoms with much less frustrated antiferromagnetic interactions are stabilized and a magnetic short-range or long-range order is developed. The system is close to the point of magnetic instability and spin fluctuations should be included to describe properties of this system.

DOI: 10.1103/PhysRevB.79.052505

PACS number(s): 74.25.Ha, 74.25.Jb

The metallic state and magnetic properties of new Fe-As based superconductors^{1,2} raised the question about the nature of magnetic interactions in these systems. Measured magnetic moments are small [$(\sim 0.3-0.8)\mu_B$] indicating that these materials most likely itinerant and are close to the nonmagnetic state. However, specific details of magnetic instabilities in these systems have not been analyzed, and so it is unclear to what extent these systems are itinerant or localized. In this Brief Report we analyze the different phases of the CaFe_2As_2 superconductor² and estimate the criteria of magnetic instability in real and reciprocal space. By comparing obtained results with similar calculations for already known magnetic systems, we provide some additional illustrations to explain why a CaFe_2As_2 system can be classified as an antiferromagnetic (AFM) system at the borderline between itinerant and localized behavior, with a degree of magnetic short-range or long-range instability determined primarily by Fe-As bonding.

The calculations have been done using local-spin-density approximation (LSDA) with full-potential linear augmented plane-wave, full-potential and atomic sphere approximation (ASA) linear muffin tin orbital methods. All electronic structure calculations are in good agreement with each other and ASA results are very close to the full-potential ones. The noninteracting susceptibility has been calculated using an ASA Green's function³ approach,

$$\chi_{ij}(\epsilon_F) = \frac{1}{\pi} \text{Tr} \text{Im} \int^{\epsilon_F} d\epsilon G_{ij}(\epsilon) G_{ji}(\epsilon), \quad (1)$$

where $G_{ij}(\epsilon)$ is the Green's function. Evidently the sum rule for the density of states (DOS) is $N_i(\epsilon) = \sum_j \chi_{ij}$ and the usual Stoner criteria for ferromagnetism (FM) is $IN(\epsilon_F) = 1$, with I being a Stoner parameter.

The local-moment criterion⁴ is written as

$$S_0 = I\chi_{00} > 1, \quad (2)$$

while criteria of the FM or AFM pair formation⁵ [short-range order (SRO) instability] are

$$S_{01}^{\pm} = I(\chi_{00} \pm \chi_{01}) > 1, \quad (3)$$

where “+” is for FM and “−” is for AFM orderings. We also use the generalized stability parameter

$$S_N = I \sum_{j=0}^N r_j \chi_{0j}, \quad (4)$$

with $r_j = “+”$ for FM orientation of moments i and j and $r_j = “−”$ for AFM orientation.

We analyze the local and nonlocal susceptibilities in real space for the presumably itinerant systems and the natural question arises: how reliably can the real-space nearest-neighbor (NN) coupling analyses predict the itinerant magnetic state? To demonstrate the applicability of such an approach, we analyze several well-known magnetic materials with a different degree of itineracy (see Table I and Fig. 1). Several typical magnetic scenarios can be identified. bcc Fe represents the relatively localized magnet with criterion (2) well satisfied (for the value of I see Ref. 6). The “itineracy” parameter $\alpha = (S_{\infty} - S_0)/S_0$ is just 0.1, so bcc Fe is a local-moment system with a well-established long-range order (LRO) [$I\chi(\mathbf{q}=0) > 1$] and small amount of itineracy. The cases of Ni, Cr, or fcc Mn are intermediate. Criterion (2) is not satisfied, while NN couplings support a developing instability against LRO appearance. These systems can be classified as “no local-moment” or strongly itinerant ($\alpha > 0.5$) systems with well-established LRO. The Mn case is special due to different results for bcc and fcc structures. We show the results for no local-moment fcc Mn ($\alpha \approx 0.15$), while bcc Mn can form local moment. The fcc Pd represents a system where local-moment instability is highly unlikely ($S_0 < 0.4$) with a large itineracy parameter $\alpha > 0.5$. NN susceptibilities, however, are also large and positive and provide a corresponding increase in the DOS at the Fermi level. Thus, the fcc Pd comes close to FM instability. The hcp Ti is also nonmagnetic and not very far from AFM instability, with large negative NN susceptibilities and all of criteria (2) and (3) are not fulfilled. All of these results are well supported by experiment and provide necessary justification of our real-space analysis in other metallic systems.

Continuing with the case of CaFe_2As_2 , Table II presents the local and nonlocal susceptibilities for the two states of CaFe_2As_2 known from the experiment as the superconducting (finite pressure) and normal (ambient pressure) phases² with corresponding distances between Fe and As atoms $R_{\text{Fe-As}}$.

TABLE I. The density of states $N(E_F)$ at the Fermi level, local and several nonlocal susceptibilities (in units of 1/Ry) in systems with different character of magnetic coupling. The data have been obtained for Ti and Co in hcp, Cr, and Fe in bcc, Mn, Ni, and Pd in fcc structures.

	Ti	Cr	Mn	Fe	Co	Ni	Pd
$N(E_F)$	13.5	10.5	21.5	43.9	31.5	56.1	32.1
χ_{00}	21.2	23.0	26.7	47.4	30.2	25.3	15.2
χ_{01}	-0.37	-1.3	-0.54	1.5	0.74	1.8	0.94
χ_{02}	-0.47	-0.12	0.04	-2.23	-0.46	0.01	0.05
χ_{03}	-0.31	-0.05	-0.11	0.27	0.18	0.32	0.14
χ_{04}	0.15	-0.08	0.15	-0.18	0.18	0.33	0.19
S_0	0.53	0.64	0.80	1.61	1.09	0.92	0.36

Table II and Fig. 2 show that CaFe_2As_2 represents a magnet at the borderline between localized and itinerant behavior. The following picture emerges from studies of nonmagnetic susceptibility in these phases. At a small $R_{\text{Fe-As}}$ (a superconducting phase with smaller volume) the condition Eq. (2) is not fulfilled with χ_{00} being nearly twice smaller than in bcc Fe (Table I). Thus the system can be classified as an itinerant system with no local moment. However, the nonlocal susceptibility of the two NNs is not small [$\alpha=(S_\infty - S_0)/S_0 \sim 0.19$; $\eta=\chi_{02}/\chi_{01} \approx 0.42$] and is negative ($\chi_{01} < 0, \chi_{02} < 0$). So, the criterion for AFM pair formation (3) along (1,0), (0,1), and (1,1) comes close to the instability threshold and the corresponding SRO can be stabilized. Simultaneously, the criterion in reciprocal space at certain points in \mathbf{q} space also appears to be close to instability (Fig. 3). The criterion of FM pair formation $S_{12}^+ < 1$ is not supported by NN coupling. FM fluctuations are thus strongly suppressed while AFM interactions are frustrated. A magnetic moment appears as a consequence of the sum of ex-

change fields from all sites, supporting the itinerant nature of this ground state. For small $R_{\text{Fe-As}}$, the frustration parameter $\eta \approx 0.4$, for intermediate $R_{\text{Fe-As}}$ $\eta \approx 0.2$, and at large $R_{\text{Fe-As}}$ it is even smaller. This is related to the small value of χ_{01} for the normal state. Such closeness to the zero (and to sign inversion) leads to large anisotropy of the NN exchange parameters in the magnetic state.^{7,8} As $R_{\text{Fe-As}}$ increases, $I\chi(\mathbf{q})$ approaches 1 for a larger region of wave vectors (Fig. 3), and with a further increase in $R_{\text{Fe-As}}$, it is fulfilled even for $\mathbf{q}=0$ (FM LRO) [for comparison see Refs. 9 and 10 for calculations of $\chi(\mathbf{q})$ and related functions in similar materials]. At this point the strong NN susceptibilities are not all negative, and this state is no longer reflecting small $R_{\text{Fe-As}}$ frustrations. The main difference between the shape of $\chi(\mathbf{q})$ in these phases is the disappearance of a maximum of $\chi(\mathbf{q})$ at \mathbf{q} corresponding to the stripe AFM structure and stabilization of the noncollinear state [Fig. 3(b)]. Our results are similar to those obtained in Ref. 10 where the susceptibility was calculated for undoped and doped cases of LaFeAsO , while our results are for CaFe_2As_2 under different pressure. Despite these differences, both calculations revealed a very similar trend: the strong stripe AFM instability for the normal phase and the instability with respect to the formation of the noncollinear state for the system where the superconductivity was observed experimentally. While the results are similar the noncollinearity in our case is somewhat stronger. This

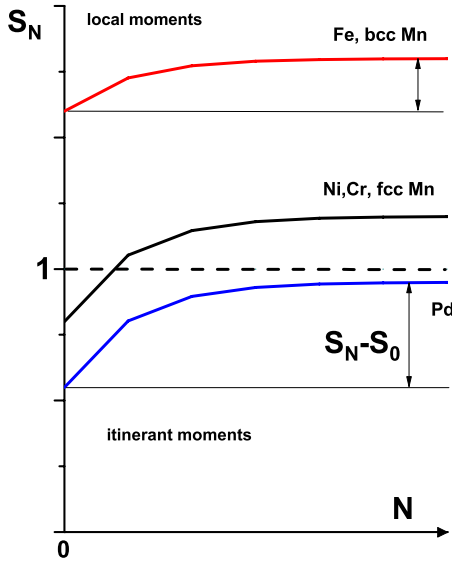


FIG. 1. (Color online) The qualitative picture of real-space criteria of magnetic state stability in different systems. The local and itinerant moment regions are shown. $N=0$ corresponds to local-moment criteria S_0 Eq. (2). S_∞ in the FM case corresponds to the regular Stoner criteria of ferromagnetism.

TABLE II. The local and nonlocal Fe atom susceptibilities (in units of 1/Ry) in CaFe_2As_2 . S : collapsed tetragonal (Ref. 2) ($R_{\text{Fe-As}}=2.336$ Å) and N : ambient pressure normal ($R_{\text{Fe-As}}=2.373$ Å) phases. Column n denotes the number of equivalent nearest neighbors. $\vec{\tau}$ is the connecting vector in units of the lattice parameter a .

	n	$\vec{\tau}$	N	S
χ_{00}	1	0,0,0	34.4	27.1
χ_{01}	4	0.5,0,0	-0.09	-0.99
χ_{02}	4	0.5,0.5,0	-0.53	-0.42
χ_{03}	4	1,0,0	0.35	0.07
χ_{04}	2	0,0,1	-0.09	-0.06
χ_{05}	8	0.5,1,0	0.12	0.16
S_0			1.17	0.92

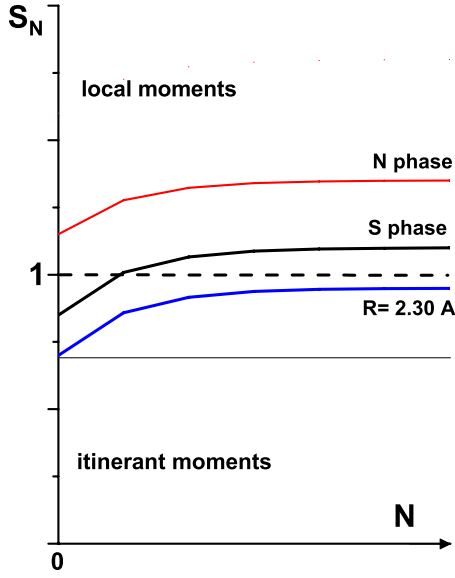


FIG. 2. (Color online) The schematic view of the real-space criteria of magnetic state stability for CaFe_2As_2 . The lower curve corresponds to structure with small $R_{\text{Fe-As}}$ (in Å), the middle curve corresponds to collapsed tetragonal (Ref. 2) ($R_{\text{Fe-As}}=2.336$ Å) phase, and the upper curve corresponds to ambient pressure normal ($R_{\text{Fe-As}}=2.373$ Å) phase.

noncollinearity is directly related to the strong coupling between moments at larger distances (beyond the first two NNs) which is very natural for the itinerant magnet. We found similar effects in Fe-Se (Ref. 8) and believe that is the generic feature of iron pnictides when the Fe moment is small.

One can parametrize the stability function $\chi(\mathbf{q})$ using only Fe-Fe χ_{ij} from Table II:

$$\begin{aligned} \chi(\mathbf{q}) = & \chi_{01}[\cos(q_x) + \cos(q_y)] + 2\chi_{02} \cos(q_x)\cos(q_y) \\ & + \chi_{03}[\cos(2q_x) + \cos(2q_y)] + \dots \end{aligned} \quad (5)$$

While this parametrization reflects many important features of total $\chi(\mathbf{q})$ from Fig. 3, it does not include, for instance, Fe-As contributions.

In both phases, the shape of the maximum of $\chi(\mathbf{q})$ is never sharp. The value $R_{\text{Fe-As}}=2.328$ Å can be considered a critical value (R_{crit}) for the local magnetic moment to be stable. The critical value R_{crit} of magnetic instability appears to be close to the R_{crit} values where the superconductivity has been observed.² At intermediate $R_{\text{Fe-As}}$ there are regions where the local moment and LRO criteria are not fulfilled while the SRO criterion for AFM pairs $S_{12}^{-1} \geq 1$. This peculiar phase of AFM NN pairs of Fe atoms exists in a very small interval of $R_{\text{Fe-As}}$. While the system is close to being classified as itinerant, the formation of magnetism is somewhat unusual. The degree of itinerancy is controlled by the competition of the strong tendency of intra-atomic exchange on the Fe atom to form localized moments (with the direct exchange coupling between them), and Fe-As bonding destroying intra-atomic magnetic instability and adding superexchange to the pool of competing interactions.⁷ The range of these interactions is about 0.5–1 eV, so smaller scale (0.1–

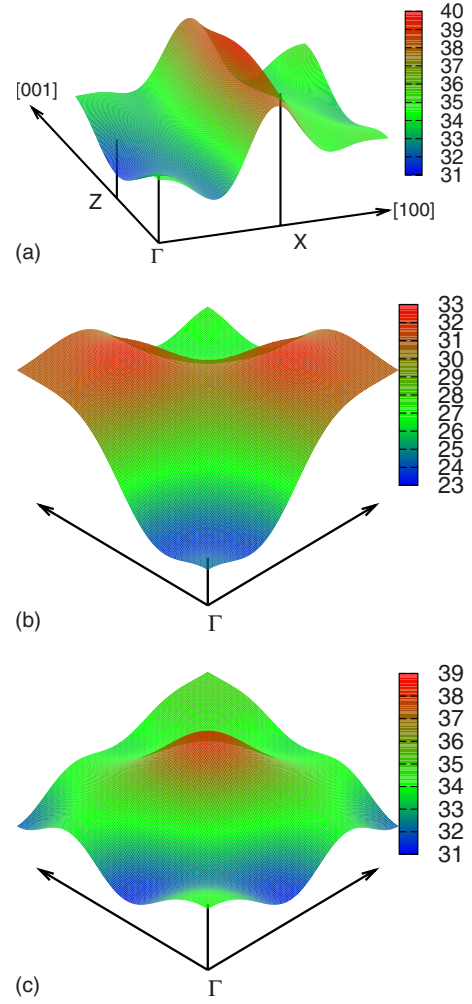


FIG. 3. (Color online) The static susceptibility $\chi(\mathbf{q})$ of CaFe_2As_2 (in $1/\text{Ry}$) for the structures corresponding to the normal and superconducting phases (Ref. 2). (a) $\chi(\mathbf{q})$ in-plane $[101]$ for the normal phase at ambient pressure. (b) $\chi(\mathbf{q})$ for collapsed (superconducting) phase (Ref. 2) ($[001]$ and $[010]$ axes are shown). (c) $\chi(\mathbf{q})$ for the normal phase at ambient pressure ($[001]$ and $[010]$ axis are shown). The stability criteria corresponds to $1/I=29.4$ Ry^{-1} (see Ref. 6). The vectors correspond to the structure rotated by 45° .

0.01 eV) spin interactions (like exchange) may have strong variations and are unlikely to produce the intrinsic set of parameters for these systems.¹¹

It is relevant to estimate how close the normal magnetic state of pnictides is to the quantum critical point. We estimated the parameter characterizing the closeness of the system to the quantum critical point (point of magnetic instability) $\delta = \chi^{-1}(\mathbf{Q}) / \max[\chi^{-1}(\mathbf{q} + \mathbf{Q}) - \chi^{-1}(\mathbf{Q})]$, where χ is a total (enhanced) magnetic susceptibility $\chi^{-1}(\mathbf{Q})$ for the observed stripe ordering. Our full-potential calculations revealed that for the magnetic state with $M=1.3\mu_B$ the parameter $\delta \approx 0.35$, while for the experimental value of $M=0.9\mu_B$ δ is 0.2, indicating that CaFe_2As_2 is rather close to the magnetic instability and for adequate description the spin fluctuations must be included. These estimations have been performed only for static susceptibility and do not include zero-point motion effects or anharmonicity of spin fluctuations, which

we believe should be important in this case. The studies of the dynamic nature of local moments will be done in our following publication.

Our calculations revealed that χ_{02} is rather stable as a function of $R_{\text{Fe-As}}$, while χ_{01} is very sensitive to that distance and even changes its sign at larger $R_{\text{Fe-As}}$. This supports the view that the crystallographic phases corresponding to normal and superconducting states of CaFe_2As_2 have very different structures of pair interactions, providing no justification for the applicability of any localized models for the entire range of observed pressures. Thus, the collapsed tetragonal (superconducting) phase is marginally itinerant no local-moment system, on the brink of an instability against forming a short-range or long-range noncollinear magnetic

order and has all the prerequisites for strong frustrations between its first two nearest neighbors, while the ambient pressure phase has a static local magnetic moment on Fe atoms with a stable short-range or long-range magnetic order of a stripe type. The system is close to the quantum critical point and spin fluctuations must be included to describe the magnetic properties of this system.

V.A. would like to thank S. Bud'ko and K. Belashchenko for continuing inspiring discussions. Work at the Ames Laboratory was supported by the U.S. Department of Energy, Basic Energy Sciences, under Contract No. DE-AC02-07CH11358.

*Current address: Materials Science and Technology Division, Oak Ridge National Laboratory, Oak Ridge, TN 37831.

¹Y. Kamihara, T. Watanabe, M. Hirano, and H. Hosono, *J. Am. Chem. Soc.* **130**, 3296 (2008).

²M. S. Torikachvili, S. L. Bud'ko, N. Ni, and P. C. Canfield, *Phys. Rev. Lett.* **101**, 057006 (2008); *Phys. Rev. B* **78**, 104527 (2008); A. Kreyssig, M. A. Green, Y. Lee, G. D. Samolyuk, P. Zajdel, J. W. Lynn, S. L. Bud'ko, M. S. Torikachvili, N. Ni, S. Nandi, J. Leao, S. J. Poulton, D. N. Argyriou, B. N. Harmon, P. C. Canfield, R. J. McQueeney, and A. I. Goldman, *Phys. Rev. B* **78**, 184517 (2008).

³M. van Schilfgaarde and V. P. Antropov, *J. Appl. Phys.* **85**, 4827 (1999); V. P. Antropov, M. van Schilfgaarde, S. Brink, and J. L. Xu, *ibid.* **99**, 08F507 (2006).

⁴P. W. Anderson, *Phys. Rev.* **124**, 41 (1961).

⁵M. Inoue and T. Moriya, *Prog. Theor. Phys.* **38**, 41 (1967).

⁶J. F. Janak, *Phys. Rev. B* **16**, 255 (1977).

⁷K. D. Belashchenko and V. P. Antropov, *Phys. Rev. B* **78**, 212505 (2008).

⁸J. J. Pulikkotil, M. van Schilfgaarde, and V. P. Antropov, arXiv:0809.0283 (unpublished).

⁹J. Dong, H. J. Zhang, G. Xu, Z. Li, G. Li, W. Z. Hu, D. Wu, G. F. Chen, X. Dai, J. L. Luo, Z. Fang, and N. L. Wang, *Europhys. Lett.* **83**, 27006 (2008); I. I. Mazin, D. J. Singh, M. D. Johannes, and M. H. Du, *Phys. Rev. Lett.* **101**, 057003 (2008); K. Kuroki, S. Onari, R. Arita, H. Usui, Y. Tanaka, H. Kontani, and H. Aoki, *ibid.* **101**, 087004 (2008).

¹⁰Y. Yanagi, Y. Yamakawa, and Y. Ono, *J. Phys. Soc. Jpn.* **77**, 123701 (2008).

¹¹P. Chandra, P. Coleman, and A. I. Larkin, *Phys. Rev. Lett.* **64**, 88 (1990).